Author Manuscript

Author Manuscript

Author Manuscript

Author Manuscript

HHS Public Access

Author manuscript

Cancer Res. Author manuscript; available in PMC 2020 June 01.

Published in final edited form as:

Cancer Res. 2019 June 01; 79(11): 2909–2922. doi:10.1158/0008-5472.CAN-18-3134.

Upregulation of PD-L1 via HMGB1-activated IRF3 and NF-κB contributes to UV radiation-induced immune suppression

Wei Wang[1,2], **Nicole M. Chapman**[3], **Bo Zhang**[1,2], **Mingqi Li**[1,2], **Meiyun Fan**[1,2], **R. Nicholas Laribee**[1,2], **M. Raza Zaidi**[4,5], **Lawrence M. Pfeffer**[1,2], **Hongbo Chi**[3], and **Zhao-Hui Wu**[1,2,*]

[1]Department of Pathology and Laboratory Medicine, University of Tennessee Health Science Center, Memphis, Tennessee

[2]Center for Cancer Research, University of Tennessee Health Science Center, Memphis, Tennessee

[3]Department of Immunology, St Jude Children's Research Hospital, Memphis, Tennessee

[4]Fels Institute for Cancer Research and Molecular Biology, Lewis Katz School of Medicine at Temple University, Philadelphia, Pennsylvania

[5]Department of Medical Genetics and Molecular Biochemistry, Lewis Katz School of Medicine at Temple University, Philadelphia, Pennsylvania.

Abstract

Solar ultraviolet radiation (UVR) suppresses skin immunity, which facilitates initiation of skin lesions and establishment of tumors by promoting immune evasion. It is unclear whether immune checkpoints are involved in the modulation of skin immunity by UVR. Here we report that UVR exposure significantly increased expression of immune checkpoint molecule PD-L1 in melanoma cells. The damage-associated molecular patterns molecule HMGB1 was secreted by melanocytes and keratinocytes upon UVR, which subsequently activated the receptor for advanced glycation endproducts (RAGE) receptor to promote NF-κB- and IRF3-dependent transcription of PD-L1 in melanocytes. UVR exposure significantly reduced the susceptibility of melanoma cells to CD8+ T cell-dependent cytotoxicity, which was mitigated by inhibiting the HMGB1/TBK1/IRF3/NF-κB cascade or by blocking the PD-1/PD-L1 checkpoint. Taken together, our findings demonstrate that UVR-induced upregulation of PD-L1 contributes to immune suppression in the skin microenvironment, which may promote immune evasion of oncogenic cells and drive melanoma initiation and progression.

Keywords

UV radiation; melanoma; immune suppression; NF-κB; IRF3; PD-L1

[*]**Corresponding author:** Zhao-Hui Wu, University of Tennessee Health Science Center, 19 S. Manassas St., Memphis, TN 38163. Phone: 901-448-2612; Fax: 901-448-3910; zwu6@uthsc.edu.

Conflict of interest: The authors declare no potential conflicts of interest.

Author Manuscript Author Manuscript Author Manuscript Author Manuscript

Introduction

Solar ultraviolet radiation (UVR) is a key epidemiological factor causing skin cancers, such as cutaneous melanoma (1). As an environmental genotoxic stressor, UVR induces DNA damage, elicits inflammation as well as alters genome structure and function in skin cells, which all contribute to the development of skin cancers and aging. Within the solar UV spectrum, UVB and UVA are of major environmental significance to skin carcinogenesis, since UVC is mostly absorbed by ozone in the earth's atmosphere. UVB can penetrate into the dermis papillary area and induce DNA damage in skin-residing keratinocytes, melanocytes and dendritic cells, resulting in its much higher carcinogenicity than UVA (2). The influence of UVR in oncogenic mutation of melanoma was further supported by the TCGA melanoma study, which identified the UVR-associated mutation signature in 76% of primary tumors and 84% of metastatic samples in melanoma patients (3). Besides leading to genomic mutation, UVR could suppress the local immune response through damaging and expelling skin Langerin^{+} antigen-presenting dendritic (Langerhans) cells. Additionally, UVR attenuates systemic immunity by inhibiting effector and memory T cells while activating regulatory T and B cells (4). The resulting immunosuppressive microenvironment of UVR-exposed skin enables premalignant skin cells and tumor cells to escape immune surveillance and facilitates cutaneous melanoma initiation and progression. Consistently, increased risk of invasive melanoma was observed in organ-transplant patients who normally underwent medical immunosuppression to prevent graft rejection (5). Therefore, reinvigorating the immunosuppressive microenvironment of the skin after UVR could play a pivotal role in reducing incidence and progression of invasive melanoma.

Recent advances in understanding the critical role of immune checkpoints in regulating tumor-infiltrating T cell activity have led to a radical shift in cancer immunotherapy and remarkable success in treating invasive melanoma patients with immune checkpoint blockers, such as humanized antibodies antagonizing cytotoxic T lymphocyte antigen 4 (CTLA4, CD152), programed death-1 (PD-1, CD279) or its ligand (PD-L1, CD274) (6). Naïve T cell activation requires T cell receptor (TCR) activation by recognition of specific antigen presented by antigen-presenting cells (APC), and costimulatory or coinhibitory signals to further modulate T cell activation (7). Costimulatory signals, such as CD28 ligation with B7–1/CD80 or B7–2/CD86, are required for effective activation of T cell immunity. On the contrary, coinhibitory signals, such as CTLA4 binding with B7–1/B7–2 and PD-1/PD-L1 ligation, function as immune checkpoints to prevent tissue damage from overactivated T cell immunity and maintain peripheral immune tolerance. Tumor cells can exploit the immune checkpoints by expressing increased ligands for coinhibitory receptors, such as PD-L1 and PD-L2, and induce an immunosuppressive tumor microenvironment, thereby escaping from anti-tumor immunity (8). Thus, blocking immune checkpoint signals mediated by CTLA4 and PD-1/PD-L1 significantly enhances anti-tumor immunity and has shown durable efficacy in treating various types of cancer, including invasive melanoma.

Although the immune suppressive effect of UVR has been well established, whether immune checkpoint activation is involved in the UVR-dependent immune suppression is not completely understood. Gene expression profiling using neonatal melanocytes from mouse skin exposed to UVR revealed an interferon response signature that includes CTLA4

Author Manuscript Author Manuscript Author Manuscript Author Manuscript

induction (9). This increased CTLA4 transcription is likely dependent on macrophage-produced IFN-γ within the skin microenvironment (9,10). Here, we show that UVB also induces PD-L1 upregulation in melanocytes and melanoma cells, which is independent of interferon signaling. Instead, UVR induces HMGB1 release from skin cells, which engages the RAGE receptor and activates the NF-κB/IRF3 transcriptional complex in melanocytes. The NF-κB/IRF3 complex was enriched on the PD-L1 promoter upon UVR and was responsible for transcriptional upregulation of PD-L1. Consistently, PD-L1 levels were significantly correlated with activation of NF-κB and IRF3 gene signature in melanoma patient samples. Moreover, blocking the HMGB1/RAGE/NF-κB/IRF3 signaling cascade or using PD-1/PD-L1 checkpoint blocker dramatically enhanced the susceptibility of melanoma cells to $CD8^+$ T cell-mediated cytotoxicity after UVR exposure. Overall, our findings support a critical role of UVR-induced PD-L1 upregulation in promoting an immunosuppressive microenvironment in the skin after UVR, which facilitates the evasion of premalignant melanocytes and melanoma cells from tumor immune surveillance, leading to melanoma initiation and progression.

Materials and Methods

Cells and Reagents

The SK-Mel-28, SK-Mel-2, MeWo, A375, HaCat and B16 cells were obtained from ATCC, and maintained in DMEM or RPMI1640 media supplemented with 10% FBS following standard culture conditions. Human primary epidermal melanocytes (HEM) were purchased from Lifeline and cultured with DermaLife Melanocyte Complete Medium following the manufacturer's protocol. The WM35 and WM1341 cell lines were generous gifts from Dr. Meenhard Herlyn (Wistar, Philadelphia, PA), and were cultured in DMEM supplemented with 10% FBS. ATCC cell lines were characterized by Short Tandem Repeat (STR) profiling, and cells resuscitated from original passage were used up to 20 passages within 6 months in all experiments. Mycoplasma contamination was routinely tested by DAPI staining. SK-Mel-28 KO lines (TBK1 KO, HMGB1 KO, RAGE KO and IRF3 KO) were generated with CRISPR/Cas9. lentiCRISPR v2 was a gift from Feng Zhang (Addgene plasmid # 52961). The sgRNA sequences used were as following: sg1TBK1 CAT AAG CTT CCT TCG TCC AG and sg2TBK1 GAA GAA CCT TCT AAT GCC TA; sg1HMGB1 GGA GAT CCT AAG AAG CCG AG and sg2HMGB1 GAG AAG TTG ACT GAA GCA TC; sg1RAGE TAT CTC CCA GGG GCA GTA GT and sg2RAGE GTG GCT CAC CCC ACA GAC TG; sg1IRF3 TTT AGC AGA GGA CCG GAG CA and sg2IRF3 ATC TAC GAG TTT GTG AAC TC.

Electrophoretic mobility super-shift assay (EMSA)

Briefly, 10 μg of total cellular extract was incubated with ^{32}P-labeled double-stranded oligonucleotides (NF-κB: 5'-TCA ACA GAG GGG ACT TTC CGA GAG GCC-3', or OCT-1: 5'-TGT CGA ATG CAA ATC ACT AGA A-3') in EMSA reaction buffer for 15 min at room temperature. The reaction was separated on a 4% non-denaturing polyacrylamide gel, which was then dried and analyzed with a Cyclone phosphoimager (PerkinElmer Life Sciences).

Author Manuscript Author Manuscript Author Manuscript Author Manuscript

Immunoprecipitation and Immunoblotting

Briefly, cells were lysed in 10% PBS and 90% IP lysis buffer (20 mM Tris (pH 7.0), 250 mM NaCl, 3 mM EDTA, 3 mM EGTA, 0.5% Nonidet P-40, 2 mM DTT, 0.5 mM PMSF, 20 mM β-glycerol phosphate, 1 mM sodium orthovanadate, 1 μg/ml leupeptin, 1 μg/ml aprotinin, 10 mM p-nitrophenyl phosphate, and 10 mM sodium fluoride). 5% of total lysates were used as input for each sample. The remaining lysate was incubated with 1 μg of primary antibody (or control IgG) on the rotator at 4 °C overnight. Protein G sepharose was then added and incubated for another 4 h at 4 °C. Protein G sepharose-enriched complexes were resolved on SDS-PAGE gels and transferred onto PVDF membranes. Protein signals were detected by specific antibodies and visualized by chemiluminescence.

Chromatin immunoprecipitation (ChIP)

In brief, cells were cross-linked with 1% formaldehyde, sonicated and then immunoprecipitated with antibodies against p65 or IRF3 in dilution buffer (1% Triton X-100, 2 mM EDTA, 150 mM NaCl, 20 mM Tris-HCl, pH 8.1). The ChIP-qPCR primers were designed to amplify the promoter regions containing respective binding sites in PD-L1 promoter. For ChIP-reChIP experiments, the p65 immunopreciptate-containing beads were washed and resuspended in reChIP buffer (dilution buffer containing 10mM DTT) and incubated at 37°C for 50 minutes. The sample was then diluted 40 times in dilution buffer, and subjected to secondary IP with anti-IRF3 antibody. Enriched chromatin was analyzed by qPCR with respective primer sets.

Conditioned media preparation and extracellular HMGB1 enrichment

Centricon-10 (Amicon, Beverly, MA) was used to concentrate the extracellular HMGB1 protein. Cell culture media (10 ml) were collected after respective treatments and applied to the concentrators followed with centrifugation at 5,000 g for 2 hours. The media fraction containing molecules larger than 10 KD (HMGB1; 25 KD) was enriched in a volume around 50 μl. The extracellular HMGB1 level was examined by western blot.

Immunofluorescence and Flow cytometry

To measure cell surface PD-L1 protein level, cultured cells were washed with PBS and incubated with recombinant human PD-1 Fc protein (R&D Systems) at room temperature for 1h. The Alexa Fluor 488-conjugate anti-human (Life Technologies) was used as secondary antibodies. After mounting, the cells were visualized using an EVOS fluorescence microscope (Thermo). To determine the PD-L1 level in cells by flow cytometry, unfixed cells were incubated with Alexa Fluor 488-conjugate PD-1 Fc protein on ice for 30 min and analyzed with Accuri 6 flow cytometer (BD Biosciences).

To prepare tumor cell suspension for flow cytometry analysis, xenograft tumors were harvested, washed extensively in PBS and minced before digestion with type IV collagenase (2 mg/ml), hyaluronidase (0.01%) and DNAse I (20 μg/ml) (Sigma-Aldrich) in HBSS at 37°C for 2h. The cell suspensions were filtered through a cell strainer (70 μm) and washed in PBS containing 2 mM EDTA and 2% FBS. Cell suspensions were then incubated with anti-CD8 (53–6.7)-FITC and anti-GZMB (GB11)-PE (all from Invitrogen) for 1h at 4 °C, and analyzed with Accuri 6 flow cytometer.

Author Manuscript Author Manuscript Author Manuscript Author Manuscript

CD8$^+$ T cell isolation and activation

Human peripheral blood mononuclear cells (PBMCs) were isolated from apheresis rings obtained from the Blood Donor Center at St. Jude Children's Hospital. Written informed consent was obtained from blood donors for their discarded blood products to be used for research purposes. This consent form has been approved by the Institutional Review Board at St. Jude Children's Research Hospital and is in accordance with the Declaration of Helsinki. The PBMC were isolated using lymphocyte separation medium and density centrifugation, and the naïve CD8$^+$ T cells were purified by magnetic beads (Miltenyi Cat #130–093-244) following the manufacturer's instructions. Polyclonal effector CD8$^+$ T cells were generated by stimulating cells with immobilized anti-CD3 (1 μg/ml; clone OKT3, Bio X Cell) and soluble anti-CD28 (2 μg/ml; clone CD28.2, Biolegend) antibodies in the presence of 100 U/ml recombinant human interleukin-2 (IL-2) for two days in complete RPMI medium containing 10% FBS and penicillin, streptomycin, and L-glutamine. Live cells were isolated using lymphocyte separation medium and density centrifugation, followed by expansion in complete medium containing IL-7 (10 ng/ml) and IL-15 (10 ng/ml) for five days.

To generate tumor-specific effector CD8$^+$ T cells (TA-CTLs), PBMCs were incubated in tissue culture-treated plates for two hours at 37 °C in complete RPMI medium. Naïve CD8$^+$ T cells were purified from the suspension cell fraction as above and rested in complete RPMI medium containing IL-7 and IL-15. The suspension cell fraction that was depleted of naïve CD8$^+$ T cells was then incubated with soluble anti-CD3 antibody (10 μg/ml) overnight to induce both T and B cell activation, which allows for B cells to serve as antigen-presenting cells (11,12). The cells were then washed and incubated for 24 hours with irradiated SK-Mel-28 melanoma cells at a 3:1 tumor cell-to-immune cells ratio. The cultures with then fixed with 1% PFA prepared in PBS for 10 min at 37 °C, followed by washing with complete RPMI medium. Naïve CD8$^+$ cells and the fixed, tumor-pulsed immune cells were then mixed at a 2:1 ratio and incubated for two days in complete RPMI 1640 medium containing soluble anti-CD28 antibody (1 μg/ml) and 100 U/ml IL-2. The live CD8$^+$ T cells were isolated using lymphocyte separation medium and expanded in completed medium containing IL-7 and IL-15 for five days.

To obtain CD8$^+$ T cells from OT-I mice, the spleen and peripheral lymph nodes (pLN) were harvested from female OT-I mice (The Jackson Laboratory), which contain T-cells whose TCRs are specific for ovalbumin peptide residues 257–264 (OVA257–264). Following manual disruption and ACK-mediated lysis of red blood cells, CD8$^+$ T cells were positively selected using CD8 microbeads (Ly-2, Miltenyi Biotech) per the manufacturer's instructions. Naïve CD8$^+$CD25$^-$CD44$^-$CD62L$^+$ OT-I cells were then sorted using a Sony Synergy. Naïve OT-I cells were suspended in complete Click's medium and activated with anti-CD3 (clone 2C11, 5 μg/ml) and anti-CD28 (5 μg/ml) antibodies in the presence of IL-2 (100 U/ml) for two days, removed from the antibodies, and expanded in IL-2-containing medium for three additional days. The cells were maintained in IL-7 and IL-15-containing medium prior to use in cytotoxicity assays or tumor experiments.

Author Manuscript Author Manuscript Author Manuscript Author Manuscript

Xenograft studies

All animal studies were conducted in accordance with NIH animal use guidelines and following protocols approved by IACUC at UTHSC. NOD.Cg *Prkdcscid Il2rgtm1Wjl*/SzJ (NSG) mice (age 6 wk) were maintained in the UTHSC animal facility. SK-Mel-28 cells (Luciferase-labeled) were treated with UVB (50 mJ/cm^2) or mock treated. After 24 h, 1×10^6 SK-Mel-28 cells and 2.5×10^6 TA-CTLs were subcutaneously co-injected into the flanks of these mice (2 per mouse, n=5 per group) following a co-transplantation model reported previously (13). Tumor volume was assessed by caliper measurement using the formula ($width^2 \times length/2$). Mice were also imaged by Xenogen IVIS system (Perkin Elmer). The mice were treated with anti-PD-1 monoclonal antibody (BioXCell, clone J116, 100 μg/mouse) or isotype on day 4 after transplantation then every other day for two weeks as indicated. At the endpoint, the mice were sacrificed and primary tumors were isolated for further analyses.

For syngeneic mouse melanoma xenograft model, C57/BL6J mice (age 7 weeks) were maintained in the UTHSC animal facility. B16-OVA cells were treated with UVB (50 mJ/cm^2) or mock treated. After 24 h, 5×10^5 B16-OVA cells and 1×10^6 OTI-$CD8^+$ T cells were subcutaneously co-injected into the flanks of C57/BL5 mice (2 per mouse, 4 male+3 female mice per group). The mice were treated with anti-PD-L1 monoclonal antibody (BioXCell, clone 10F.9G2, 100 μg/mouse) or isotype on day 1 after transplantation then every other day for two weeks as indicated. Tumor growth was monitored by caliper measurement and harvest tumors were analyzed as above.

Results

UV radiation induces PD-L1 upregulation in melanoma cells in a NF-κB-dependent manner.

UVB radiation enhances the expression of the immune checkpoint molecule CTLA4 in melanocytes in neonatal mouse skin, which is dependent on macrophage-secreted IFN-γ within the skin microenvironment upon UVR (9,10). We further analyzed the melanocytic gene expression profile and revealed that another immune checkpoint molecule PD-1 ligand (PD-L1/CD274) was also significantly upregulated following UVB exposure (Supplementary Fig. S1A). To determine whether UVR influenced the expression of PD-L1 in melanoma cells, we treated SK-Mel-28 cells with UVB. Expression of PD-L1 was significantly increased at both the mRNA and protein levels in response to UVB treatment (Fig. 1A). UVB exposure increased PD-L1 levels in SK-Mel-28 cells in a time-dependent manner (Supplementary Fig. S1B). Consistently, PD-L1 level on cell surface also was substantially increased in SK-Mel-28 cells upon UVB exposure (Fig. 1B-C). UVB exposure also increased the expression of PD-L1 in a panel of human melanoma cell lines and mouse B16 melanoma cells (Fig. 1D), suggesting that PD-L1 induction is a conserved stress response to UV exposure in melanocytes and melanoma cells.

In the tumor microenvironment, PD-L1 expression can be induced by inflammatory cytokines such as interferon (IFN)-γ (6), which activates STAT1 and increases PD-L1 transcription (14). We found PD-L1 induction by UVB was not affected by momelotinib (CYT387, JAK1/2 inhibitor) or WP1066 (JAK2 inhibitor), although UVB-induced activation

Author Manuscript Author Manuscript Author Manuscript Author Manuscript

of STAT1 and STAT3 was blocked (Supplementary Fig. S1C), suggesting IFN-γ likely is dispensable for UVB-induced PD-L1 in melanoma cells. UVR also activates the transcription regulator NF-κB, which was suggested to be a downstream mediator of IFNγ-induced PD-L1 induction (15). We observed that UVB treatment induced NF-κB activation in melanoma cells (SK-Mel-28, WM35 and WM1341), melanocytes (human epidermal melanocytes/HEM) and keratinocytes (HaCaT) in a dose-dependent manner (Fig. 1E and Supplementary Fig. S1D-E). NF-κB has been reported to upregulate PD-L1 transcription in ovarian, lung and breast cancer cells (16–18). Indeed, we found that UVB-induced PD-L1 upregulation in melanoma cells was blocked by an IKK2 inhibitor TPCA-1 (Supplementary Fig. S1F). Moreover, depletion of RelA/p65 of NF-κB family remarkably attenuated PD-L1 induction in SK-Mel-28 cells exposed to UVB (Fig. 1F-G, compare blue and green lines). All these data suggested that UVB-induced NF-κB activation plays a critical role in mediating PD-L1 induction in melanoma cells.

UVB-induced NF-κB activation depends on TBK1 and IKK

NF-κB activation by UVR, especially by UVC, depends on casein kinase 2 (CK2)-mediated p38α activation, which in turn phosphorylates IκBα and promotes its degradation (19). However, inhibiting either p38 or CK2 minimally affected NF-κB activation in UVB-treated melanoma cells (Supplementary Fig. S2A). We previously reported that UVC-induced NF-κB activation was regulated by DNA damage response kinases ATM and ATR (20,21). Nevertheless, inhibiting ATM, ATR or DNA-PK with specific inhibitors or by genetic deletion did not substantially affect UVB-induced NF-κB activation (Supplementary Fig. S2B-D). IκBα kinases (IKK) were shown to be required for UV-induced NF-κB activation (20,22,23), and we found IKK inhibition, by either a pharmacological inhibitor or genetic deletion, abrogated NF-κB activation by UVB (Fig. 2 A-B), supporting an essential role of IKKs in mediating UVB-induced NF-κB signaling. Supershift analysis further revealed that the p65/p50 heterodimer was the major NF-κB complex activated by UVB in SK-Mel-28 melanoma cells (Supplementary Fig. S2E). Since IKK activity is required for UVB-induced NF-κB activation, we examined whether the IKK upstream kinase TAK1 is required for this signaling cascade. Surprisingly, depletion of TAK1 barely affected UVB-induced phosphorylation of IκBα and p65, suggesting that TAK1 is not essential for IKK activation in response to UVB (Supplementary Fig. S2F).

TBK1 was originally identified as a TRAF2/TANK-associated kinase activating NF-κB (24). We found inhibiting TBK1 abolished UVB-induced NF-κB activation, which was comparable to that by inhibiting IKK (Fig. 2A). TBK1-dependent phosphorylation of IKKβ was reported to activate canonical IKK activity by directly phosphorylating IKKβ (25). In accordance, we found that UVB-activated TBK1 phosphorylates IKKβ *in vitro*, which depends on TBK1 kinase activity (Fig. 2C). UVB treatment induced a dose-dependent activation of TBK1 and phosphorylation of its canonical downstream substrate IRF-3 (Supplementary Fig. S2G). Moreover, UVB-induced p65 phosphorylation was abolished in TBK1-knock out (KO) SK-Mel-28 cells (Fig. 2D). PD-L1 induction by UVB was also inhibited in IKKα/β$^{-/-}$ MEFs, TBK1-KO cells, and cells co-treated with inhibitors of IKK or TBK1 (Fig. 2A–2D), supporting that IKK and TBK1 are essential for UVB-induced NF-κB activation and subsequent PD-L1 induction.

Author Manuscript Author Manuscript Author Manuscript Author Manuscript

HMGB1 secretion upon UVB is required for NF-κB activation.

We next asked whether TBK1/NF-κB activation by UVB depends on a signal from the extracellular milieu after UVB treatment. We found conditioned media (CM) from UVB-treated SK-Mel-28 cells could activate NF-κB, which was mediated by TBK1 and IKK, but not CK2 (Fig. 3A). CM from UVB-treated primary melanocytes also effectively induced NF-κB activation in cells that were not exposed to UVB (Fig. 3B), suggesting that secreted molecule(s) in CM from UVB-treated cells is sufficient for inducing NF-κB activation. Moreover, this activity was sensitive to heat inactivation but not nuclease treatment, suggesting that secreted proteins are essential for NF-κB activation upon UVB (Fig. 3B).

Secretion of the nuclear protein HMGB1, as a DAMP (danger-associated molecular patterns) molecule, from keratinocytes has been linked with skin inflammation upon UVR (26,27). We found HMGB1 was released from melanocytes and melanoma cells as early as 0.5 h after UVB exposure (Fig. 3C, Supplementary Fig. S2H). The increased extracellular HMGB1 was likely due to active secretion instead of passive release from necrotic cells, since little cell necrosis was observed until 2 h after UVB radiation. The subcellular translocation and release of HMGB1 was further confirmed by immunofluorescence showing a substantial decrease of nuclear HMGB1 in response to UVB (Fig. 3D). To determine if HMGB1 is essential for UVB-induced NF-κB activation in melanoma cells, we generated HMGB1-KO SK-Mel-28 cells. Deletion of HMGB1 abolished the activation of TBK1 and phosphorylation of p65 and IRF-3 in response to UVB (Fig. 3E). Moreover, CM from UVB-treated HMGB1-KO SK-Mel-28 cells failed to activate NF-κB in parental SK-Mel-28 cells (Fig. 3F). These results strongly support that HMGB1 secretion upon UVB exposure plays a critical role in mediating NF-κB activation in an autocrine and/or paracrine fashion.

To determine if HMGB1 is sufficient for activating NF-κB in melanoma cells, we treated SK-Mel-28 cells with recombinant human HMGB1 (rHMGB1). NF-κB activation was substantially increased in SK-Mel-28 cells exposed to rHMGB1 (Fig. 3G). Moreover, treatment with recombinant HMGB1-BoxA fragment, which serves as an inactivating competitor for the HMGB1 receptor (28), decreased UVB-induced NF-κB activation in melanoma cells in a dose-dependent manner (Fig. 3H). Importantly, PD-L1 induction was detected in melanoma cells exposed to UVB CM from wide type (WT) SK-Mel-28 cells, but not from HMGB1-KO SK-Mel-28 cells, likely due to inability to induce NF-κB activation (Fig. 3I).

SIRT1 inactivation by UVB promotes HMGB1 secretion

Active secretion of HMGB1 has been associated with increased HMGB1 acetylation at its nuclear localization signals, which blocks the re-entry of shuttling HMGB1 into the nucleus (29). We found UVB treatment significantly increased HMGB1 acetylation (Supplementary Fig. S3A). Moreover, depletion of the deacetylase SIRT1 further enhanced UVB-induced HMGB1 acetylation (Supplementary Fig. S3B), which is consistent with previous reports showing that SIRT1-dependent deacetylation inhibits HMGB1 secretion (30,31). Accordingly, deletion of SIRT1 further enhanced UVB-induced TBK1 activation and subsequent phosphorylation of IRF3 and p65 (Supplementary Fig. S3C). We found the

Author Manuscript Author Manuscript Author Manuscript Author Manuscript

interaction between HMGB1 and SIRT1 was decreased in response to UVB treatment (Supplementary Fig. S3D). Inhibiting SIRT1 activity by nicotinamide (NAM) promoted HMGB1 secretion from SK-Mel-28 cells, comparable to that by UVB treatment (Supplementary Fig. S3E). Moreover, WT SIRT1, but not the catalytic-inactive H355A mutant, suppressed UVB-induced TBK1/NF-κB activation in melanoma cells (Supplementary Fig. S3F). We also found treatment with the SIRT1 activating agent, resveratrol, inhibited HMGB1 secretion by UVB (Supplementary Fig. S3G), which was correlated with decreased TBK1 activation and reduced phosphorylation of IRF3 and p65 in cells exposed to UVB (Supplementary Fig. S3H). SIRT1 is a NAD-dependent deacetylase and decreased NAD^+/NADH ratio suppresses SIRT1 function (32). We found that the intracellular NAD^+/NADH ratio was significantly decreased in SK-Mel-28 cells in response to UVB (Supplementary Fig. S3I), which may be responsible for decreased SIRT1 activity upon UVB exposure. All these results indicate that UVR may promote HMGB1 acetylation and secretion by suppressing SIRT1 in melanoma cells, which results in increased activation of NF-κB/IRF3.

RAGE mediates HMGB1-induced TBK1/ NF-κB activation upon UVB

To identify the receptor responsible for HMGB1-induced NF-κB activation upon UVB exposure, we treated SK-Mel-28 cells with UVB in the presence of inhibitors of Toll-like receptor 4 (TLR4) or RAGE (receptor for advanced glycation endproducts). Inhibiting RAGE with FPS-ZM1 abolished UVB-induced NF-κB activation to a similar extend as inhibition of either IKKβ or TBK1, while treatment with TLR4 inhibitor had little effect (Fig. 4A). Inhibiting RAGE also abrogated UVB-induced TBK1/NF-κB activation and IRF3 phosphorylation in another melanoma cell line MeWo (Fig. 4B). UVB-induced TBK1/NF-κB activation was absent in RAGE-KO SK-Mel-28 cells (Fig. 4C). Inhibiting RAGE also blocked NF-κB activation by CM from UVB-treated melanoma cells (Fig. 4D). Moreover, the CM from UVB-treated melanoma cells failed to induce TBK1/ NF-κB activation in RAGE-KO cells, although the same CM was able to induce TBK1/ NF-κB activation in HMGB1-KO cells (Fig. 4E). In accordance, UVB-induce PD-L1 upregulation was also diminished by RAGE inhibition (Fig. 4B and 4F) or in RAGE-KO SK-Mel-28 cells (Supplementary Fig. S4A). These data support an essential role of RAGE in mediating the HMGB1-induced activation of NF-κB and IRF3.

IRF3 and NF-κB form a complex on the PD-L1 promoter and enhance its transcription

It was recently reported that NF-κB activation by TNFα could increase PD-L1 levels by stabilizing PD-L1 protein, which depends on upregulation of the deubiquitinase CSN5 and subsequent deubiquitination of PD-L1 (33). PD-L1 mRNA levels were not significantly changed in breast cancer cells treated with TNFα. In contrast, we found UVB exposure significantly increased PD-L1 mRNA expression (Fig. 1A), which was attenuated by inhibiting RAGE, IKK or TBK1 (Fig. 5A). The increased PD-L1 transcription by UVB was also diminished in HMGB1-KO cells (Fig. 5B), suggesting that UVB/HMGB1-activated NF-κB directly enhanced PD-L1 transcription. Accordingly, we detected a substantial enrichment of RelA/p65 on the PD-L1 promoter region upon UVB exposure (Fig. 5C), which supports a role of NF-κB in upregulating PD-L1 transcription in melanoma cells after UVR.

Author Manuscript Author Manuscript Author Manuscript Author Manuscript

Interestingly, we found UVB-induced PD-L1 upregulation was also decreased in IRF3-KO melanoma cells (Fig. 5D) or cells transfected with IRF3-targeting siRNAs, in which UVB-induced TBK1/NF-κB activation was not affected (Supplementary Fig. S4B). This observation indicates that UVB-activated NF-κB may not be sufficient for upregulating PD-L1 in melanoma cells, and IRF3 also plays an important role in mediating PD-L1 induction by UVB. Scanning the promoter sequence of PD-L1 revealed two putative IRF-binding sites (ISRE) along with the NF-κB-binding site within the proximal region of PD-L1 promoter. We also detected significantly increased IRF3 binding at the distal ISRE2 site within the PD-L1 promoter upon UVB (Fig. 5E). Unexpectedly, UVB-induced IRF3 enrichment was also detected at NF-κB-binding site in the promoter, while p65 recruitment was specifically at NF-κB-binding site upon UVB exposure. To determine the importance of ISRE2 and NF-κB-binding site in regulating PD-L1 transcription upon UVB, we generated a luciferase reporter whose transcription was controlled by the PD-L1 promoter. We found deletion of ISRE2 did not significantly reduce the reporter activity in response to UVB, whereas mutating NF-κB-binding site diminished UVB-induced transactivation (Fig. 5F), supporting an essential role of the NF-κB-binding site in enhancing PD-L1 transcription upon UVB. IRF3 was previously showed to interact with NF-κB/p65, and the IRF3-p65 complex was required for transactivation of IRF3-target genes such as interferon induction by LPS (34). We confirmed that IRF3 and p65 formed a complex in melanoma cells treated by UVB (Fig. 5G). Moreover, we found the p65-IRF3 complex was enriched on the NF-κB-binding site in the PD-L1 promoter in response to UVB exposure (Fig. 5H), suggesting that UVB-induced transactivation of PD-L1 was regulated by p65-IRF3 regulatory complex.

UVB-induced PD-L1 upregulation inhibited cytotoxic T cell-mediated anti-melanoma immunity

Coinhibitory signals from PD-1/PD-L1 keep T cells activity in check and attenuate cytotoxic $CD8^+$ T cell (CTL)-mediated tumoricidal effects (6). We found that UVB treatment significantly reduced susceptibly of SK-Mel-28 (Fig. 6A) or B16 melanoma cells (Supplementary Fig. S5A) to CTL-dependent cytotoxicity. The decreased CTL-susceptibility was observed in SK-Mel-28 cells exposed to CTLs cells activated by either anti-CD3/CD28 antibodies (Supplementary Fig. S5B, AA T cells, black lines) or tumor-specific antigens from IR-inactivated melanoma cells (Supplementary Fig. S5B, TA T cells, red lines). Inhibiting RAGE or TBK significantly increased the specific lysis of UVB-exposed melanoma cells by CTLs (Fig. 6B). Moreover, depletion of IRF3 also enhanced the susceptibility of melanoma cells to CTL-mediated cytotoxicity after UVB exposure (Fig. 6C). Blocking PD-L1/PD-1 signaling with an anti-PD-1 antibody significantly decreased survival of UVB-treated SK-Mel-28 cells co-cultured with activated CTLs (Fig. 6D), which was associated with dramatically increased CTL-dependent cytolysis in UVB-reposed melanoma cells (Fig. 6E). These findings suggest that UVB-induced activation of TBK1/IRF3/NF-κB promotes melanoma cell escape from CTL-mediated anti-melanoma immunity by upregulating PD-L1.

To determine whether the level of PD-L1 correlates with NF-κB activation and/or IRF3 activity in melanoma patient samples, we analyzed the genomic data from the TCGA-cutaneous melanoma study (3). We found the PD-L1/CD274 expression level is significantly

Author Manuscript Author Manuscript Author Manuscript Author Manuscript

correlated with NF-κB-p65-pS536 levels, a surrogate of NF-κB activity, determined by RPPA in melanoma patients (Fig. 6F, Supplementary Fig. S5C). Since IRF3 was not included in the RPPA analyses, we used an IRF3-upregulated gene signature (35) as a readout for measuring IRF3 activity in the patient samples. High IRF3 activity in melanoma patient samples was also correlated with PD-L1/CD247 transcription level (Fig. 6F, 6G), supporting a critical role of IRF3 activation in promoting PD-L1 expression.

UVB promotes melanoma evasion from CTL-mediated immunity by upregulating PD-L1

To determine whether UVB exposure promotes melanoma growth by escaping anti-melanoma immunity, we stimulated human $CD8^+$ T cells with inactivated SK-Mel-28 cells. UVB treatment of tumor antigen-activated CTLs had little effect on their cytotoxicity towards SK-Mel-28 cells in vitro, while UVB exposure of the SK-Mel-28 cells decreased their cytotoxicity (Supplementary Fig. S6A). Following a co-transplantation animal model using melanoma cells and human tumor reactive T cells (13), we co-injected SK-Mel-28 cells, exposed to UVB or mock-treated, with or without activated CTLs into the flanks of immunodeficient NSG mice. As expected, activated CTLs dramatically suppressed SK-Mel-28 xenograft tumor growth (Fig. 7A-C). Consistent with our in vitro results, UVB exposure substantially enhanced SK-Mel-28 xenograft growth in the presence of tumor reactive CTLs, which was attenuated by anti-PD1 treatment (Fig. 7A-C). These data suggested that upregulation of PD-L1 in melanoma cells by UVB could suppress the tumoricidal activity of CTLs to promote melanoma progression. Indeed, we detected substantially increased expression of PD-L1 in xenografts from UVB-treated melanoma (Fig. 7D-E), which correlated with increased TBK1/IRF3/NF-κB activation in these tumors (Fig. 7D). CTLs cytotoxicity against melanoma cells, visualized by Granzyme B staining and quantified by percentage of $GZMB^+$ cells in the $CD8^+$ population isolated from tumors, was significantly suppressed in SK-Mel-28 tumors exposed to UVB, which was reinvigorated by an-PD1 treatment (Supplementary Fig. S6B, Fig. 7F). Moreover, injection of PD-1 antibody did not suppress TBK1/IRF3/ NF-κB activation by UVB and consequent PD-L1 induction (Fig. 7D-7E), suggesting that the improved tumor regression by anti-PD1 was mediated by improved CTL activity. Consistent results were also observed in a syngeneic B16 melanoma xenograft model, in which UVB exposure substantially decreased the susceptibility of B16-OVA melanoma to activated OVA-specific OTI-CTLs (Supplementary Fig. S6C). In accordance to SK-Mel-28 xenograft model, treatment with anti-PD-L1 antibody significantly enhanced CTL-dependent antitumor immunity while minimally affecting UVB-induced TBK1/IRF3/ NF-κB signaling (Supplementary Fig. S6D, S6E) in B16-OVA tumors.

We also compared the growth of xenograft tumors from UVB-treated WT or IRF3-KO SK-Mel-28 cells co-transplanted with tumor reactive CTLs. Although both of these cells were exposed to UVB, IRF-3 deficiency significantly reduced tumor growth (Supplementary Fig. S6F), likely owing to increased melanoma sensitivity to CTL-mediated anti-melanoma immunity. Consistent with this notion, PD-L1 levels in IRF3-KO SK-Mel-28 xenograft tumors were substantially decreased compared to that in wild type xenografts (Supplementary Fig. S6G, S6H). Taken together, our results support that UVB-induced

Author Manuscript Author Manuscript Author Manuscript Author Manuscript

IRF3/NF-κB activation promotes melanoma cells evasion from CTL-mediated anti-tumor immunity, which is dependent on the upregulation of PD-L1.

Discussion

UVR-induced immune suppression plays critical roles in promoting skin cancer (36). UVB-dependent expulsion of Langerhans cells from the skin microenvironment substantially reduces the antigen-presenting capacity of the skin-resident dendritic cells, which facilitates the premalignant cells and early stage melanoma cells to escape from tumor immune surveillance (36,37). UVB also induces immunosuppressive cytokine production from keratinocytes, such as IL-4, IL-10, and prostaglandin (PGE2). Moreover, exposure of UVB enhances migration of UVR-damaged Langerhans cells into the regional lymph nodes, which induces the expansion of regulatory T cells and reduces effector and memory T cells, resulting in systemic inhibition of adaptive immunity (4,37). Here we showed that UVB also increased expression of PD-L1 in melanocytes and melanoma cells, which could facilitate pre-malignant and melanoma cells to inhibit effector T cell activity, thereby reducing anti-tumor immunity in the skin microenvironment. Moreover, PD-L1 has been shown to be present on the surface of the exosomes secreted from tumor cells, which are found in the circulation and are expected to suppress T cell activity systemically (38). Therefore, PD-L1 induction in skin cells may participate in local and systemic immune suppression by UVR, and could play an important role in immune evasion of melanoma cells from tumor immune surveillance (Fig. 7G). Targeting UVB-induced HMGB1/RAGE/TBK1 signaling could abrogate PD-L1 induction in melanocytes and melanoma cells exposed to UVB, which may serve as potential pharmacological targets for mitigating immune escape of the premalignant melanocytes from immune surveillance.

Our previous studies have shown that transcription factor NF-κB can be activated by a variety of genotoxic agents in human cancer cells (39,40). As a DNA damaging agent, UVC has been shown to activate NF-κB in a p38 and CK2-dependent manner (19). Moreover, we found that UVC-induced NF-κB activation was also regulated by the DNA damage response kinases ATM and ATR (20,21). Inhibition of ATM or ATR could suppress or augment UVC-induced NF-κB activation, respectively. In contract to UVC, our data indicated that UVB-induced NF-κB activation in human keratinocytes and melanoma cells was not affected by inhibiting p38/CK2 or by ATM/ATR deletion. Moreover, another upstream kinase TAK1, which we have previously shown to be essential for DNA damage-induced NF-κB signaling (41), was dispensable for UVB-induced NF-κB activation in skin cells. All these data suggest that UVB could activate NF-κB in skin cells through a distinct signaling cascade. Indeed, we found HMGB1, secreted from skin cells as a stress response to UVR, was essential for NF-κB activation by UVB exposure. UVB-enhanced HMGB1 acetylation, which was mediated by inactivation of SIRT1, may play an essential role in promoting HMGB1 secretion from the skin cells. In the skin microenvironment, HMGB1 binds to the DAMP receptor RAGE and leads to downstream kinase TBK1 activation, which is required for UVB-induced NF-κB activation. Consistent with previous studies (22,23,42), IKKβ was required for UVR-induced NF-κB activation. There was strong evidence that IKKs are indispensable for UVR-induced IκB proteolysis, as UV-induced IκBα degradation and NF-κB activation were not detected in IKK-KO cells, particularly in IKKβ-deficient ($IKK\beta^{-/-}$)

Author Manuscript Author Manuscript Author Manuscript Author Manuscript

cells. Besides phosphorylating IκBα in cytoplasm, the nuclear IKKβ also functions as an adaptor protein for IκBα association with β-TrCP in the nucleus which results in IκBα degradation and subsequent NF-κB activation in response to UVR (42). Furthermore, computational modeling also suggested that constitutive phosphorylation of IκBα by basal IKK activity, which affects the turnover rate of IκBα, and IκBα synthesis inhibition are crucial for UV-induced NF-κB activation (23,43). We found UVB-activated TBK1 could directly phosphorylate IKKβ, which may promote IKK activation. TBK1-dependent phosphorylation of IKKβ was reported to either activate or inhibit canonical IKK activity depending on the upstream stimuli (25,44). In skin cells exposed to UVB, TBK1 activity is essential for IKK activation and subsequent NF-κB activation. It remains to be further delineated how RAGE promotes TBK1 activation in cells exposed to UVB. Nevertheless, our findings demonstrated that UVB activates NF-κB in skin cells through a signaling pathway initiated from the cell surface receptor RAGE and HMGB1 stimulation from the skin microenvironment, which is distinct from the atypical nucleus-to-cytoplasm NF-κB activation signaling utilized by other genotoxic agents, including UVC.

A number of transcriptional regulators have been shown to modulate PD-L1 expression. In the tumor microenvironment, PD-L1 can be induced by inflammatory cytokines such as IFN-γ, which induces activation of STAT1 and increased PD-L1 transcription (6,14). Other transcriptional regulators, including HIF-1, Myc, STAT3, AP-1 and NF-κB, have also been shown to enhance PD-L1 transcription in response to a variety of upstream signals (45). Additionally, NRF2 was recently reported to be required for UVR-induced PD-L1 upregulation in primary melanocytes and keratinocytes isolated from the human skin (46). Our data indicated that PD-L1 induction by UVB was minimally affected in NRF2-depleted human melanoma cells examined, suggesting a potential cell-type specific mechanism for regulating PD-L1 transcription in primary cells. We found NF-κB, in association with IRF3, plays an essential role in enhancing PD-L1 transcription in melanoma cells upon UVB. Also, NF-κB and IRF3 were indispensable for PD-L1 upregulation by UVB in primary melanocytes, in which they may mediate PD-L1 transcription with NRF2 alternatively and/or collaboratively. Besides directly promoting PD-L1 gene transcription, NF-κB has been shown to indirectly stabilize PD-L1 by upregulating the deubiquitinase CSN5, which inhibits the ubiquitination and proteasomal degradation of PD-L1 in breast cancer cells (33). We showed that, in melanoma cells, both the mRNA and protein levels of PD-L1 were increased after UVR. Moreover, the increased PD-L1 transcription by UVR was attenuated by inhibiting NF-κB upstream kinases IKKβ or TBK1. We further confirmed the enrichment of NF-κB on the PD-L1 promoter in melanoma cells after UVR. All these findings support that UVB-induced NF-κB activation directly increases PD-L1 transcription in melanocytes and melanoma cells.

Intriguingly, we found IRF3 also play a critical role in promoting PD-L1 induction by UVR by forming a transcriptional complex with NF-κB/p65. To our knowledge, the transcriptional regulatory role for IRF3 in PD-L1 expression has not been reported. A recent study showed that DNA damage-induced PD-L1 upregulation in breast cancer cells was regulated in a STING-dependent manner (47). As the primary downstream transcriptional regulator of STING, IRF3 likely plays a role in regulating PD-L1 transcription in breast cancer cells treated with chemotherapeutic drugs. Furthermore, our previous studies

Author Manuscript Author Manuscript Author Manuscript Author Manuscript

demonstrated that NF-κB is activated upon chemotherapeutic treatment in breast cancer cells (48). It is tempting to speculate that NF-κB may also collaborate with IRF3 in promoting PD-L1 transcription in breast cancer cells treated with chemotherapeutics. IRF3 was previously showed to interact with NF-κB/p65, and the IRF3-p65 complex was required for transactivation of IRF3-target genes in response to LPS (33). In UVB-treated melanocytes, IRF3 was recruited onto the NF-κB-binding site within PD-L1 promoter through association with p65, which coordinately promoted PD-L1 transcription. The finding that the upstream kinase TBK1 is responsible for activation of both NF-κB and IRF3 upon UVR may have provided an attractive pharmacological target for antagonizing PD-L1 induction by UVR by simultaneously blocking the activation of NF-κB and IRF3.

Cancer immune surveillance plays an essential role in preventing tumor incidence and effectively eliminates oncogenic cells at precancerous stages (8). Therefore, the occurrence of many cancers can be considered a breach of immune control, which is fueled by additional oncogenic mutations. The immune suppressive landscape caused by UVR provides a permissive environment for premalignant cells to escape from tumor immunity and promote skin cancer initiation and progression. In addition to the well-established local and systemic immune suppressive mechanisms by UVR (4), our studies indicated that activating PD-1/PD-L1 immune checkpoints by upregulating PD-L1 in melanocytes and melanoma cells also play an essential role in facilitating immune evasion of malignant skin cells from tumor immunity. Genome-wide examination of neonatal melanocytes after UVR identified an interferon gene signature, which promotes melanocytic cell survival and immune evasion (9). Secretion of HMGB1 from skin cells in response to UVR may promote an immunosuppressive microenvironment by activating PD-1/PD-L1 checkpoint, along with other previously reported immune-suppressive cytokines, such as IL-4, IL-10, PGE2 and TGFβ. Our data indicates that blocking PD-1/PD-L1 significantly enhanced $CD8^+$ T cell-mediated anti-tumor immunity against melanoma cells after UVB exposure, suggesting that immune checkpoint blockers may also mitigate UVR-promoted immune evasion during melanoma development. Treatment with anti-PD-1 blocking antibody has been shown to increase the number of $CD8^+$ memory T cells in the tumor microenvironment (49). Using small molecules, such as BMS-202 (50), that inhibit the PD-1/PD-L1 interaction may serve as an immune prevention approach to mitigate immune suppression by UVR, increase effector and memory T cell skin infiltration, and antagonize oncogenic cell immune evasion, thereby preventing the initiation and progression of invasive melanoma after UVR.

Supplementary Material

Refer to Web version on PubMed Central for supplementary material.

Acknowledgements

We thank Dr. Francesca-Fang Liao for providing SIRT1 plasmids. This work was supported in part by the National Cancer Institute (R01 CA149251), American Cancer Society (RSG-13–186-01-CSM), NGS and CORNET awards from UTHSC.

Author Manuscript Author Manuscript Author Manuscript Author Manuscript

References

1. Schulman JM, Fisher DE. Indoor ultraviolet tanning and skin cancer: health risks and opportunities. Curr Opin Oncol 2009;21:144–9 [PubMed: 19532016]
2. Cooper SJ, Bowden GT. Ultraviolet B regulation of transcription factor families: roles of nuclear factor-kappa B (NF-kappaB) and activator protein-1 (AP-1) in UVB-induced skin carcinogenesis. Current cancer drug targets 2007;7:325–34 [PubMed: 17979627]
3. Cancer Genome Atlas N. Genomic Classification of Cutaneous Melanoma. Cell 2015;161:1681–96 [PubMed: 26091043]
4. Kripke ML. Reflections on the field of photoimmunology. The Journal of investigative dermatology 2013;133:27–30 [PubMed: 22854621]
5. Robbins HA, Clarke CA, Arron ST, Tatalovich Z, Kahn AR, Hernandez BY, et al. Melanoma Risk and Survival among Organ Transplant Recipients. The Journal of investigative dermatology 2015;135:2657–65 [PubMed: 26270022]
6. Boussiotis VA. Molecular and Biochemical Aspects of the PD-1 Checkpoint Pathway. N Engl J Med 2016;375:1767–78 [PubMed: 27806234]
7. Chen L, Flies DB. Molecular mechanisms of T cell co-stimulation and co-inhibition. Nat Rev Immunol 2013;13:227–42 [PubMed: 23470321]
8. Schreiber RD, Old LJ, Smyth MJ. Cancer immunoediting: integrating immunity's roles in cancer suppression and promotion. Science 2011;331:1565–70 [PubMed: 21436444]
9. Zaidi MR, Davis S, Noonan FP, Graff-Cherry C, Hawley TS, Walker RL, et al. Interferon-gamma links ultraviolet radiation to melanomagenesis in mice. Nature 2011;469:548–53 [PubMed: 21248750]
10. Mo X, Zhang H, Preston S, Martin K, Zhou B, Vadalia N, et al. Interferon-gamma Signaling in Melanocytes and Melanoma Cells Regulates Expression of CTLA-4. Cancer Res 2018;78:436–50 [PubMed: 29150430]
11. Xia CQ, Peng R, Chernatynskaya AV, Yuan L, Carter C, Valentine J, et al. Increased IFN-alpha-producing plasmacytoid dendritic cells (pDCs) in human Th1-mediated type 1 diabetes: pDCs augment Th1 responses through IFN-alpha production. J Immunol 2014;193:1024–34 [PubMed: 24973447]
12. Lapointe R, Bellemare-Pelletier A, Housseau F, Thibodeau J, Hwu P. CD40-stimulated B lymphocytes pulsed with tumor antigens are effective antigen-presenting cells that can generate specific T cells. Cancer Res 2003;63:2836–43 [PubMed: 12782589]
13. Stewart R, Morrow M, Hammond SA, Mulgrew K, Marcus D, Poon E, et al. Identification and Characterization of MEDI4736, an Antagonistic Anti-PD-L1 Monoclonal Antibody. Cancer Immunol Res 2015;3:1052–62 [PubMed: 25943534]
14. Loke P, Allison JP. PD-L1 and PD-L2 are differentially regulated by Th1 and Th2 cells. Proc Natl Acad Sci U S A 2003;100:5336–41 [PubMed: 12697896]
15. Gowrishankar K, Gunatilake D, Gallagher SJ, Tiffen J, Rizos H, Hersey P. Inducible but not constitutive expression of PD-L1 in human melanoma cells is dependent on activation of NF-kappaB. PLoS One 2015;10:e0123410 [PubMed: 25844720]
16. Bouillez A, Rajabi H, Jin C, Samur M, Tagde A, Alam M, et al. MUC1-C integrates PD-L1 induction with repression of immune effectors in non-small-cell lung cancer. Oncogene 2017;36:4037–46 [PubMed: 28288138]
17. Xue J, Chen C, Qi M, Huang Y, Wang L, Gao Y, et al. Type Igamma phosphatidylinositol phosphate kinase regulates PD-L1 expression by activating NF-kappaB. Oncotarget 2017;8:42414–27 [PubMed: 28465490]
18. Peng J, Hamanishi J, Matsumura N, Abiko K, Murat K, Baba T, et al. Chemotherapy Induces Programmed Cell Death-Ligand 1 Overexpression via the Nuclear Factor-kappaB to Foster an Immunosuppressive Tumor Microenvironment in Ovarian Cancer. Cancer Res 2015;75:5034–45 [PubMed: 26573793]
19. Kato T, Delhase M, Hoffmann A, Karin M. CK2 is a C-terminal I kappa B kinase responsible for NF-kappa B activation during the UV response. Molecular Cell 2003;12:829–39 [PubMed: 14580335]

Author Manuscript Author Manuscript Author Manuscript Author Manuscript

20. Tan G, Niu J, Shi Y, Ouyang H, Wu ZH. NF-kappaB-dependent microRNA-125b up-regulation promotes cell survival by targeting p38alpha upon ultraviolet radiation. J Biol Chem 2012;287:33036–47 [PubMed: 22854965]
21. Wu ZH, Miyamoto S. Induction of a pro-apoptotic ATM-NF-kappaB pathway and its repression by ATR in response to replication stress. EMBO J 2008;27:1963–73 [PubMed: 18583959]
22. Huang TT, Feinberg SL, Suryanarayanan S, Miyamoto S. The zinc finger domain of NEMO is selectively required for NF-kappa B activation by UV radiation and topoisomerase inhibitors. Mol Cell Biol 2002;22:5813–25 [PubMed: 12138192]
23. O'Dea EL, Kearns JD, Hoffmann A. UV as an amplifier rather than inducer of NF-kappaB activity. Mol Cell 2008;30:632–41 [PubMed: 18538661]
24. Pomerantz JL, Baltimore D. NF-kappaB activation by a signaling complex containing TRAF2, TANK and TBK1, a novel IKK-related kinase. EMBO J 1999;18:6694–704 [PubMed: 10581243]
25. Tojima Y, Fujimoto A, Delhase M, Chen Y, Hatakeyama S, Nakayama K, et al. NAK is an I kappa B kinase-activating kinase. Nature 2000;404:778–82 [PubMed: 10783893]
26. Johnson KE, Wulff BC, Oberyszyn TM, Wilgus TA. Ultraviolet light exposure stimulates HMGB1 release by keratinocytes. Arch Dermatol Res 2013;305:805–15 [PubMed: 23942756]
27. Bald T, Quast T, Landsberg J, Rogava M, Glodde N, Lopez-Ramos D, et al. Ultraviolet-radiation-induced inflammation promotes angiotropism and metastasis in melanoma. Nature 2014;507:109–13 [PubMed: 24572365]
28. Musumeci D, Roviello GN, Montesarchio D. An overview on HMGB1 inhibitors as potential therapeutic agents in HMGB1-related pathologies. Pharmacology & therapeutics 2014;141:347–57 [PubMed: 24220159]
29. Bonaldi T, Talamo F, Scaffidi P, Ferrera D, Porto A, Bachi A, et al. Monocytic cells hyperacetylate chromatin protein HMGB1 to redirect it towards secretion. EMBO J 2003;22:5551–60 [PubMed: 14532127]
30. Rabadi MM, Xavier S, Vasko R, Kaur K, Goligorksy MS, Ratliff BB. High-mobility group box 1 is a novel deacetylation target of Sirtuin1. Kidney international 2015;87:95–108 [PubMed: 24940804]
31. Xu W, Lu Y, Yao J, Li Z, Chen Z, Wang G, et al. Novel role of resveratrol: suppression of high-mobility group protein box 1 nucleocytoplasmic translocation by the upregulation of sirtuin 1 in sepsis-induced liver injury. Shock (Augusta, Ga) 2014;42:440–7
32. Guarente L, Picard F. Calorie restriction--the SIR2 connection. Cell 2005;120:473–82 [PubMed: 15734680]
33. Lim SO, Li CW, Xia W, Cha JH, Chan LC, Wu Y, et al. Deubiquitination and Stabilization of PD-L1 by CSN5. Cancer Cell 2016;30:925–39 [PubMed: 27866850]
34. Wietek C, Miggin SM, Jefferies CA, O'Neill LA. Interferon regulatory factor-3-mediated activation of the interferon-sensitive response element by Toll-like receptor (TLR) 4 but not TLR3 requires the p65 subunit of NF-kappa. J Biol Chem 2003;278:50923–31 [PubMed: 14557267]
35. Grandvaux N, Servant MJ, tenOever B, Sen GC, Balachandran S, Barber GN, et al. Transcriptional profiling of interferon regulatory factor 3 target genes: direct involvement in the regulation of interferon-stimulated genes. J Virol 2002;76:5532–9 [PubMed: 11991981]
36. Schwarz T, Beissert S. Milestones in photoimmunology. The Journal of investigative dermatology 2013;133:E7–E10
37. Elmets CA, Cala CM, Xu H. Photoimmunology. Dermatologic clinics 2014;32:277–90, vii [PubMed: 24891051]
38. Chen G, Huang AC, Zhang W, Zhang G, Wu M, Xu W, et al. Exosomal PD-L1 contributes to immunosuppression and is associated with anti-PD-1 response. Nature 2018;560:382–6 [PubMed: 30089911]
39. McCool KW, Miyamoto S. DNA damage-dependent NF-kappaB activation: NEMO turns nuclear signaling inside out. Immunol Rev 2012;246:311–26 [PubMed: 22435563]
40. Wu ZH, Miyamoto S. Many faces of NF-kappaB signaling induced by genotoxic stress. Journal of molecular medicine 2007;85:1187–202 [PubMed: 17607554]

Author Manuscript Author Manuscript Author Manuscript Author Manuscript

41. Wu ZH, Wong ET, Shi Y, Niu J, Chen Z, Miyamoto S, et al. ATM- and NEMO-dependent ELKS ubiquitination coordinates TAK1-mediated IKK activation in response to genotoxic stress. Mol Cell 2010;40:75–86 [PubMed: 20932476]

42. Tsuchiya Y, Asano T, Nakayama K, Kato T, Karin M, Kamata H. Nuclear IKK beta Is an Adaptor Protein for I kappa B alpha Ubiquitination and Degradation in UV-Induced NF-kappa B Activation. Molecular Cell 2010;39:570–82 [PubMed: 20797629]

43. Wu S, Tan M, Hu Y, Wang JL, Scheuner D, Kaufman RJ. Ultraviolet light activates NFkappaB through translational inhibition of IkappaBalpha synthesis. J Biol Chem 2004;279:34898–902 [PubMed: 15184376]

44. Clark K, Takeuchi O, Akira S, Cohen P. The TRAF-associated protein TANK facilitates cross-talk within the IκB kinase family during Toll-like receptor signaling. Proc Natl Acad Sci U S A 2011;108:17093–8 [PubMed: 21949249]

45. Chen J, Jiang CC, Jin L, Zhang XD. Regulation of PD-L1: a novel role of pro-survival signalling in cancer. Ann Oncol 2016;27:409–16 [PubMed: 26681673]

46. Zhu B, Tang L, Chen S, Yin C, Peng S, Li X, et al. Targeting the upstream transcriptional activator of PD-L1 as an alternative strategy in melanoma therapy. Oncogene 2018;37:4941–54 [PubMed: 29786078]

47. Parkes EE, Walker SM, Taggart LE, McCabe N, Knight LA, Wilkinson R, et al. Activation of STING-Dependent Innate Immune Signaling By S-Phase-Specific DNA Damage in Breast Cancer. J Natl Cancer Inst 2017;109

48. Wang W, Mani AM, Wu ZH. DNA damage-induced nuclear factor-kappa B activation and its roles in cancer progression. J Cancer Metastasis Treat 2017;3:45–59 [PubMed: 28626800]

49. Ribas A, Shin DS, Zaretsky J, Frederiksen J, Cornish A, Avramis E, et al. PD-1 Blockade Expands Intratumoral Memory T Cells. Cancer Immunol Res 2016;4:194–203 [PubMed: 26787823]

50. Zak KM, Grudnik P, Guzik K, Zieba BJ, Musielak B, Domling A, et al. Structural basis for small molecule targeting of the programmed death ligand 1 (PD-L1). Oncotarget 2016;7:30323–35 [PubMed: 27083005]

Author Manuscript Author Manuscript Author Manuscript Author Manuscript

Significance: Findings identify PD-L1 as a critical component of UV-induced immune suppression in the skin, which facilitates immunoevasion of oncogenic melanocytes and development of melanoma.

Author Manuscript Author Manuscript Author Manuscript Author Manuscript

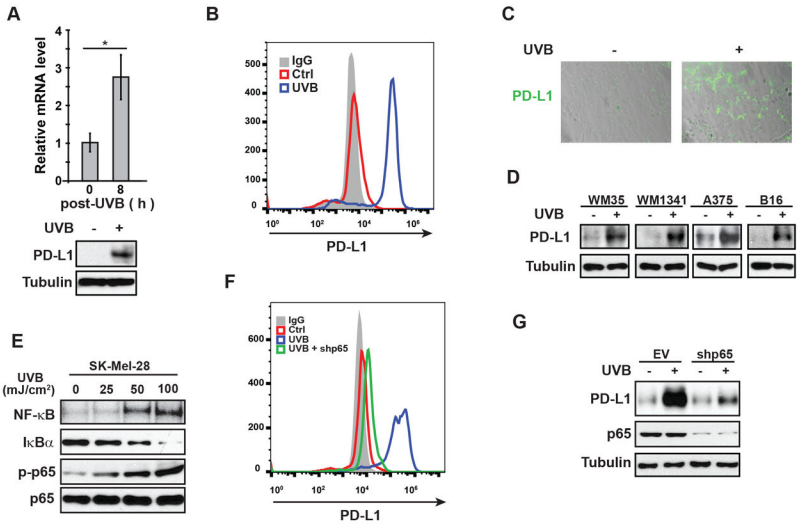

Figure 1. UVR increases PD-L1 expression in melanoma cells in a NF-κB-dependent manner.

(A-C) SK-Mel-28 cells were treated with UVB (50 mJ/cm^2). **(A)** Cells were harvested at 8 h after UVR, and expression of PD-L1 was examined by qPCR and western blot. **(B)** After 24 h, cells were analyzed by flow cytometry to determine cell surface expression of PD-L1. **(C)** Cell-surface expression of PD-L1 on SK-Mel-28 cells were visualized by binding of PD-1/Fc protein which was labeled by anti-Fc-Alexa 488 antibody. **(D)** WM35, WM1341, A357 and B16 cell lines were treated with UVB (50 mJ/cm^2). After 24 h, the expression of PD-L1 was determined by western blot. **(E)** SK-Mel-28 cells were treated with increasing doses of UVB as shown. After 4 h, EMSA and western blot were performed to examine the activation of NF-κB. **(F, G)** SK-Mel-28 cells transfected with control or p65-targeting shRNA (shp65) were exposed to UVB (50 mJ/cm^2). After 24 h, PD-L1 expression was examined by flow cytometry (F) and western blot (G). *: $p<0.05$

Author Manuscript Author Manuscript Author Manuscript Author Manuscript

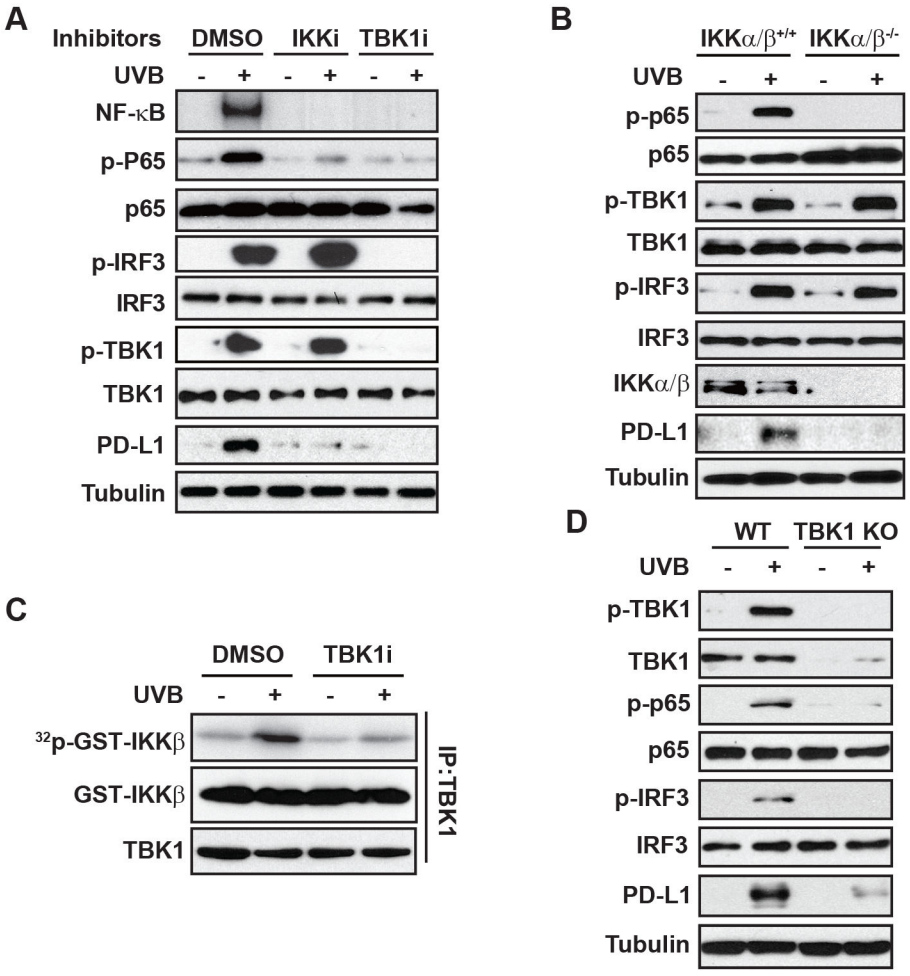

Figure 2. UVB-activated NF-κB depends on IKK and TBK1.

(A) SK-Mel-28 cells were pre-treated with the IKK inhibitor TPCA-1 (1 μM, IKKi) and TBK1 inhibitor Amlexanox (20 μM, TBKi), and then were exposed to UVB (50 mJ/cm^2). After 4 h, the cell lysates were examined by EMSA (NF-κB) and western blot as indicated. **(B)** Wild-type (IKKα/β$^{+/+}$) or IKKα/β-deficient (IKKα/β$^{-/-}$) MEFs were treated with UVB (50 mJ/cm^2), and the activation of NF-κB, TBK1 and IRF3 was examined by western blots. **(C)** SK-Mel-28 cells were exposed to UVB (50 mJ/cm^2) with or without TBK1i. Cells were harvested at 4 h after UVR, TBK1 was immunoprecipitated (IP) and used for TBK1 kinase assay with GST-IKKβ as substrate. **(D)** WT and TBK1-knockout (KO) SK-Mel-28 cells were treated and analyzed as in (B).

Author Manuscript Author Manuscript Author Manuscript Author Manuscript

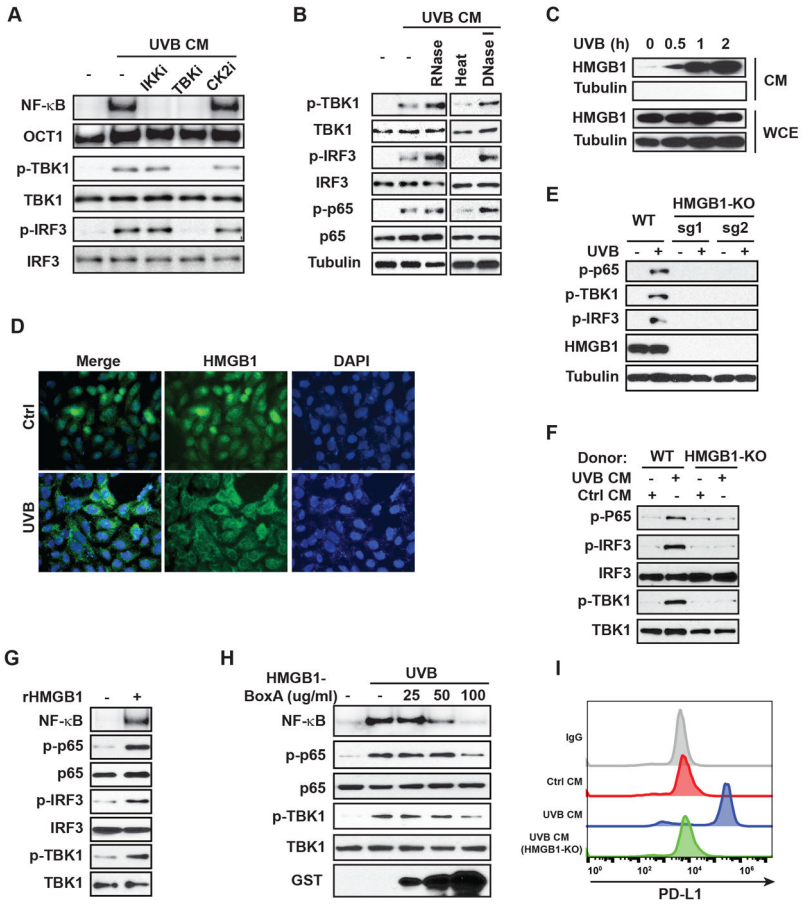

Figure 3. UVR-induced HMGB1 secretion is required for NF-κB activation by UVB.

(A) Conditioned media (CM) from SK-Mel-28 cells treated with UVB (50 mJ/cm^2) or mocked treated were collected at 4 h after exposure. Fresh SK-Mel-28 cells were incubated with CM with or without inhibitors of IKKβ (TPCA-1, IKKi), TBK1 (Amlexanox, TBKi) or CK2 (TBB, CK2i) as shown for 4 h. Then, cells were harvested and analyzed with EMSA (NF-κB) or western blot. **(B)** Conditioned media from human epidermal melanocytes (HEM) were harvested at 4 h after UVB (50 mJ/cm^2) exposure and treated as indicated before adding to fresh HEM culture. HEM cells were harvested at 4 h after CM incubation and whole-cell extracts were analyzed by western blotting with the indicated antibodies. **(C)** SK-Mel-28 cells were treated by UVB (50 mJ/cm^2). CM and whole-cell extracts (WCE) of treated cells were harvested at the times as shown, and western blotting with the indicated antibodies was performed. **(D)** HaCat keratinocytes were treated with UVB (50 mJ/cm^2) and fixed at 2 h after treatment. The Intracellular localization of HMGB1 was visualized by anti-HMGB1 antibody with immunofluorescence. Nuclei were stained with DAPI. **(E)** Parental (WT) and HMGB1-knockout (KO) SK-Mel-28 cells generated with two different sgRNAs for CRISPR were treated with UVB (50 mJ/cm^2). Whole-cell lysates were analyzed by western blot with indicated antibodies. **(F)** CM from parental (WT) or HMGB1-KO SK-Mel-28 cells with or without UVB treatment were collected. Fresh SK-Mel-28 cells were incubated with indicated CM for 4 h and whole-cell lysates were analyzed by western blot. **(G)** SK-Mel-28 cells were treated with recombinant HMGB1 (1 μg/ml) as shown. Cells were

Author Manuscript Author Manuscript Author Manuscript Author Manuscript

harvested at 4 h after treatment and analyzed with EMSA (NF-κB) or western blot. **(H)** SK-Mel-28 cells were treated by UVB (50 mJ/cm^2) with or without inactivating HMGB1-BoxA fragment at indicated doses. Cells were harvested at 4 h after treatment and whole-cell lysates were analyzed with EMSA (NF-κB) or western blot with indicated antibodies. **(I)** SK-Mel-28 cells were incubated with CM from WT or HMGB1-KO cells treated by UVB or mock treated as shown. After 24 h, PD-L1 expression was examined by flow cytometry.

Author Manuscript Author Manuscript Author Manuscript Author Manuscript

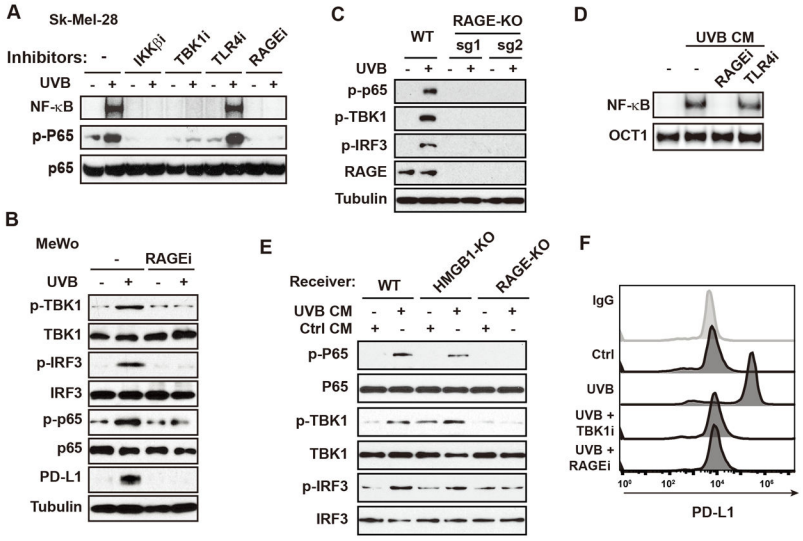

Figure 4. RAGE is required for HMGB1-promoted NF-κB/IRF3 activation in response to UVB.

(A) SK-Mel-28 cells were treated by UVB (50 mJ/cm^2) with or without inhibitors of IKKβ (TPCA-1, IKKi), TBK1 (Amlexanox, TBK1i), TLR4 (CLI-095, 1 μg/ml, TLR4i) and RAGE (FPS-ZM1, 10 μM, RAGEi). Cells were harvested at 4 h after treatment and analyzed with EMSA (NF-kB) or western blot. **(B)** MeWo cells were treated by UVB (50 mJ/cm^2) with or without RAGEi. Cells were harvested at 4 h after treatment and analyzed with western blot as shown. **(C)** RAGE-knockout (KO) SK-Mel-28 cells generated by CRISPR/Cas9 using two different sgRNAs and parental cells were treated by UVB (50 mJ/cm^2). Whole-cell lysates were analyzed by western blot with indicated antibodies. **(D)** SK-Mel-28 cells were incubated with UVB-conditioned media (CM) along with indicated inhibitors for 4 h. Whole-cell lysates were analyzed with EMSA. **(E)** CM were harvested from SK-Mel-28 cells treated with or without UVB. Parental (WT), HMGB1-KO and RAGE-KO SK-Mel-28 cells were incubated with indicated CM for 4 h, and whole-cell lysates were analyzed by western blot with indicated antibodies. **(F)** SK-Mel-28 cells treated by UVB (50 mJ/cm^2) along with inhibitors as indicated. Cell were analyzed by flow cytometry for PD-L1 expression at 24 h after the treatment.

Author Manuscript Author Manuscript Author Manuscript Author Manuscript

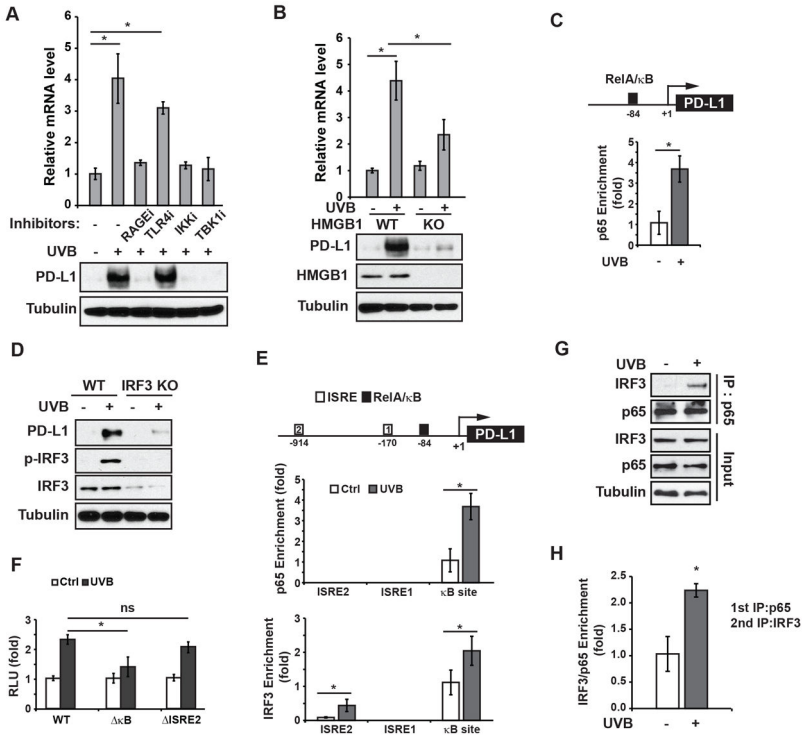

Figure 5. PD-L1 induction by UVB depends on NF-κB and IRF3.

(A) SK-Mel-28 cells were exposed to UVB with or without indicated inhibitors. After 24 h, the expression of PD-L1 was examined by qPCR and western blots. **(B)** Relative PD-L1 mRNA levels were measured in wild-type (WT) and HMGB1-knockout (KO) SK-Mel-28 cells after UVB exposure. Whole-cell extracts were analyzed by western blots. **(C)** UVB-induced enrichment of p65 in the PD-L1 promoter region was determined by chromatin immunoprecipitation (ChIP). **(D)** The PD-L1 expression level was analyzed in WT and IRF3-KO SK-Mel-28 cells after UVB exposure by western blot as in (B). **(E)** UVB-induced enrichment of p65 and IRF3 on respective ISRE and NF-κB (κB) sites within the PD-L1 promoter region was determined by ChIP. **(F)** PD-L1 promoter reporters with or without indicated motif deletion were transfected into SK-Mel-28 cells. The UVB-induced reporter activity was measured by luciferase assay. **(G)** SK-Mel-28 cells were treated with UVB (50 mJ/cm^2). Cells were harvested at 4 h after treatment and the interaction of p65 and IRF3 was analyzed with co-IP. **(H)** ChIP/ReChIP assay was conducted by sequential IP with p65 (1st IP) and IRF3 (2nd IP) antibodies. Enrichment of p65/IRF3 complex on PD-L1 promoter region was determined by qPCR. *: p<0.05, ns: not significant.

Author Manuscript Author Manuscript Author Manuscript Author Manuscript

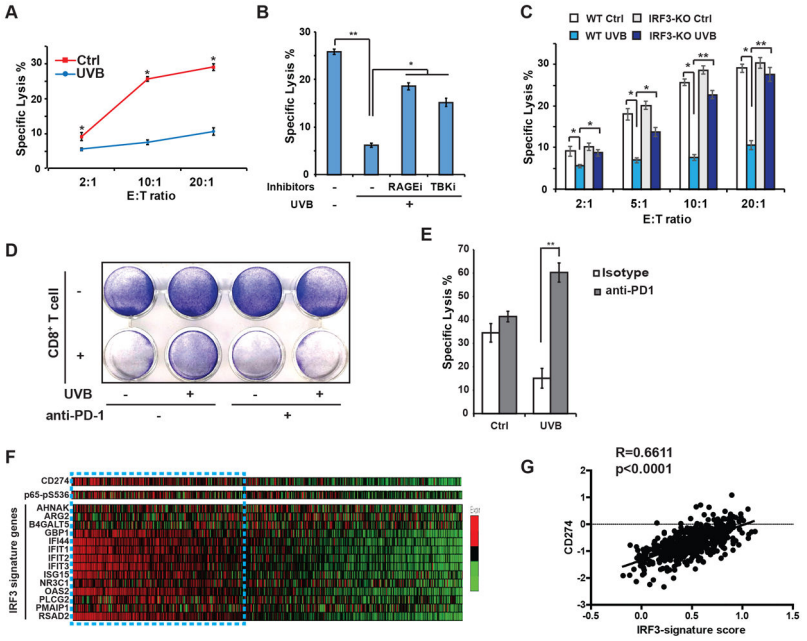

Figure 6. PD-L1 induction by UVR decreases melanoma cell susceptibility to CTL toxicity.

(A) T-cell killing assay was performed using CD3/CD28 antibody-activated human $CD8^+$ T cells (effector, E) and SK-Mel-28 cells (target, T, mock treated (red line) or UVB-exposed (blue line)) at indicated E:T ratios. Cytotoxicity was quantified by LDH assay. **(B, C)** Similar T-cell killing assays as in (A) were performed using SK-Mel-28 cells treated by UVB (50 mJ/cm^2) with or without inhibitors for TBK1 (TBKi) or RAGE (RAGEi) as shown (B), or using parental (WT) or IRF3-knockout (KO) SK-Mel-28 cells with (UVB) or without (Ctrl) UVB treatment as indicated (C). Cytotoxicity was quantified by LDH assay. **(D)** SK-Mel-28 cells treated with UVB (50 mJ/cm^2) or mock treated were cocultured with antibody-activated $CD8^+$ T cells at E:T ratio of 1:20, in the presence of anti-PD-1 (1 μg) or isotype control antibodies. Cell survival was visualized at 3 days after co-culture using crystal violet staining. **(E)** T-cell killing assays as in (A) were carried out using SK-Mel-28 cells treated by UVB (50 mJ/cm^2) with or without anti-PD-1 (1 μg) or isotype control antibodies. **(F)** RNA-seq and RPPA (p65-pS536) data from melanoma patients were retrieved from TCGA. Levels of CD274, p65-pS536 and IRF3 activation signature genes were shown with heatmap. **(G)** Gene-wise z-score was calculated in each patient sample and the sum of genes in the refined IRF3 signature gene list was used to characterize IRF3 signature score. Correlation between CD274 levels and IRF3 signature scores were determined by Pearson's correlation analyses. *: $p<0.05$; **: $p<0.01$.

Author Manuscript Author Manuscript Author Manuscript Author Manuscript

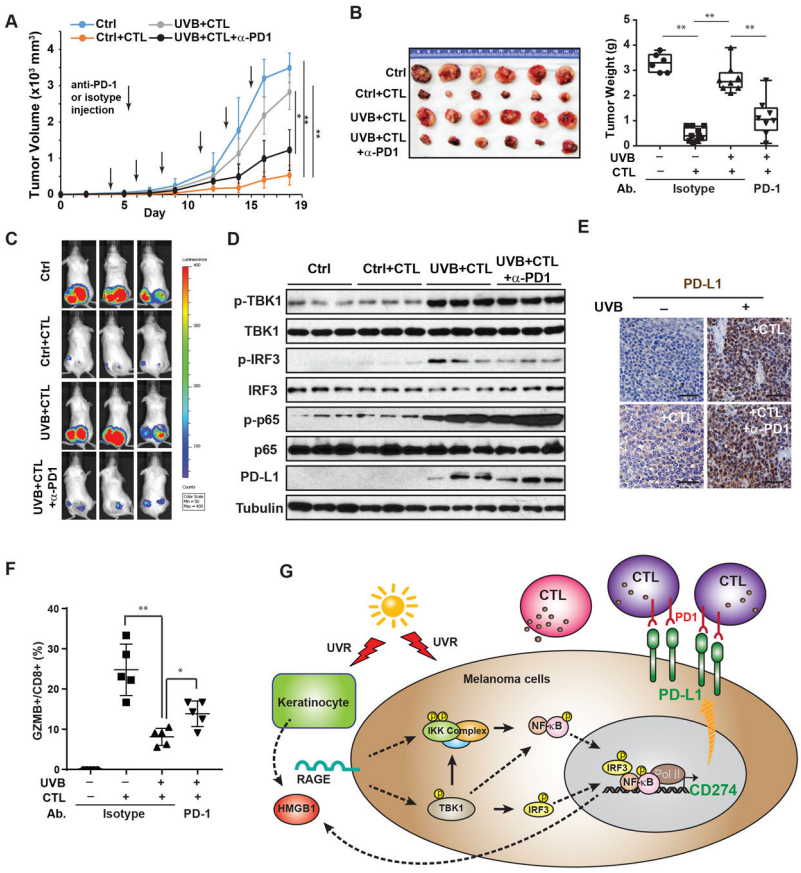

Figure 7. Blocking PD-1/PD-L1 checkpoint enhances CTL-dependent anti-melanoma immunity after UVR.

(A) SK-Mel-28-Luc cells treated with UVB or mock treated were co-transplanted with tumor-antigen-specific $CD8^+$ T cells/CTLs as indicated (n=5 per group). Mice with xenograft tumors were treated with anti-PD1 (100 μg/mouse) or isotype control antibodies as shown. Tumor growth was measured by calipers. The blue line shows tumors resulting from SK-Mel-28-Luc cells not receiving UVB and transplanted without CTLs. **(B)** Images of xenograft tumors (left) and tumor weights (right) harvested at end point. **(C)** Tumor growth on day 18 was monitored by IVIS imaging. **(D)** Lysates from tumor samples (3 per group) were analyzed by western blot with the indicated antibodies. **(E)** PD-L1 expression in xenograft tumors were determined by IHC. Scale bar: 20 μm. **(F)** Percentage of Granzyme B ($GZMB^+$) positive cell in $CD8^+$ cell population isolated from xenograft tumors of respective group were quantified by flow cytometry. **(G)** A model illustrating UVR-induced PD-L1 upregulation through activating NF-κB and IRF3, which facilitates melanoma cell immune evasion. *: $p<0.05$; **: $p<0.01$.